GENERAL ATOMIC

DIVISION OF **GENERAL DYNAMICS**

GA-4495

A PROGRAM OF BASIC RESEARCH ON MECHANICAL PROPERTIES OF REACTOR MATERIALS

QUARTERLY PROGRESS REPORT FOR THE PERIOD ENDING JUNE 30, 1963

Contract AT(04-3)-167
Project Agreement No. 4
U.S. Atomic Energy Commission

August 30, 1963

GENERAL ATOMIC
DIVISION OF
GENERAL DYNAMICS

JOHN JAY HOPKINS LABORATORY FOR PURE AND APPLIED SCIENCE
P.O. BOX 608. SAN DIEGO 12. CALIFORNIA

GA-4495

A PROGRAM OF BASIC RESEARCH ON MECHANICAL PROPERTIES OF REACTOR MATERIALS

QUARTERLY PROGRESS REPORT FOR THE PERIOD ENDING JUNE 30, 1963

Contract AT(04-3)-167
Project Agreement No. 4
U. S. Atomic Energy Commission

Work done by:

T. A. Trozera
D. Crie
P. W. Flynn
R. H. Chambers
H. Harper
J. Schultz
G. Alefeld
J. Filloux
T. Firle
L. C. Foster
D. F. Stoneburner
J. L. White

Report written by:

T. A. Trozera
R. H. Chambers
D. F. Stoneburner
J. L. White

August 30, 1963

PREVIOUS REPORTS IN THIS SERIES

GA-3376 April, May, June, 1962

GA-3585—Summary report of work from October 1, 1961, through September 30, 1962

GA 3845—October, November, December, 1962

GA-4227—January, February, March, 1963

I. DEFORMATION MECHANISMS IN BCC METALS

DEFORMATION AND FABRICATION CHARACTERISTICS OF REACTOR MATERIALS

A previous quarterly report(1) presented observations made on tantalum single crystals using etch-pit techniques and transmission microscopy. The use of etch-pit techniques has not been continued because of the necessity of thermally pinning dislocations in order to make them visible to the etchant. This introduces a possibility for rearrangement and in any case clouds the interpretation of results obtained by this method.

Thin-film microscopy of rolled single crystals has been extended, and a number of additional interesting observations have been made. The results presented previously indicated an abnormally low density of dislocations after a room-temperature deformation of ~90%. At that time no evidence for formation of sub-boundaries had been noted. Figure 1 is a light micrograph of a rolled specimen, and an area almost devoid of slip markings can be seen. Areas of this type are quite numerous, and our present feelings are that the original observations of low dislocation density could easily have resulted from viewing a region like this. Also to be noted in Fig. 1 is a distribution of slip lines, many of which have a 1- to 2-μ spacing. Figures 2 and 3 are transmission micrographs illustrating what may well be surface slip lines. A number of observations of this type have been made. It is interesting to note the dense tangles separated by a small area relatively dislocation-free. This type of artifact has also been reported on by Greenfield and Wilsdorf(2) from studies on irradiated copper. Also visible (arrows) in Fig. 3 are tracks of dislocations which have moved during observation. As can be noted, the tracks follow only a general direction, with considerable deviations, which indicates the considerable ease with which cross slipping occurs. Visual observation of moving dislocations confirms results of others with respect to the jerky motion which appears to be almost random.

A portion of the specimen used in Figs. 2 and 3 was annealed in air at 400°C for 8 hr. This thermal treatment was calculated to introduce sufficient oxygen through the specimen to pin all the dislocations present. Figures 4 and 5 are typical transmission photographs of this sample, with a corresponding selected area diffraction (S. A. D.) photo for Fig. 4. It is immediately obvious that some changes have occurred, probably as a result of the thermal treatment. The structure is almost characteristic of a cold-worked polycrystalline material, as evidenced by the S. A. D. photo. The

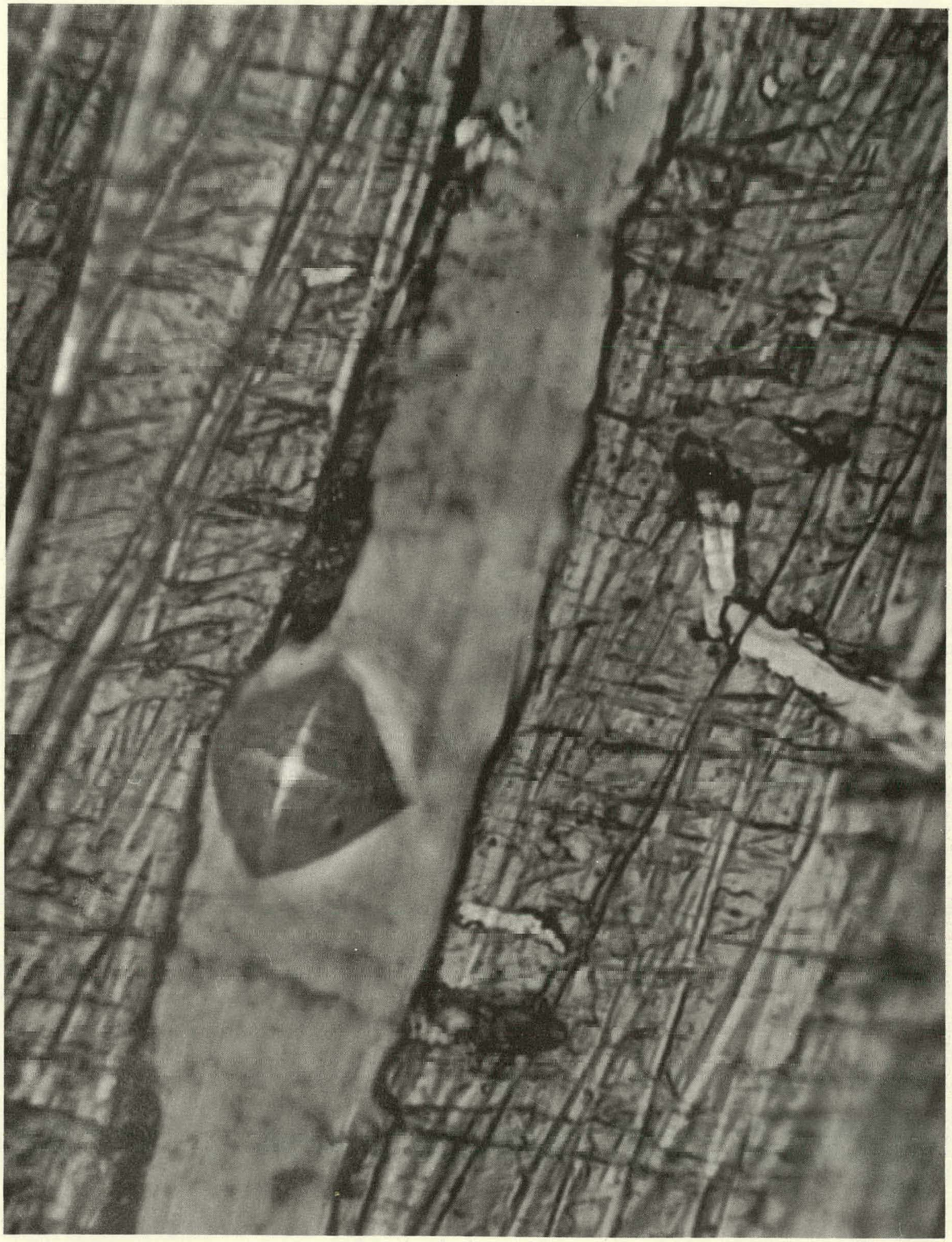

M3305-4-1

Fig. 1--Light micrograph of rolled tantalum single crystal showing area almost free of slip markings

P2064 (×~60,000)

Fig. 2--Transmission micrograph of rolled tantalum single crystal

P2071 (×~60,000)

Fig. 3--Transmission micrograph of rolled tantalum single crystal

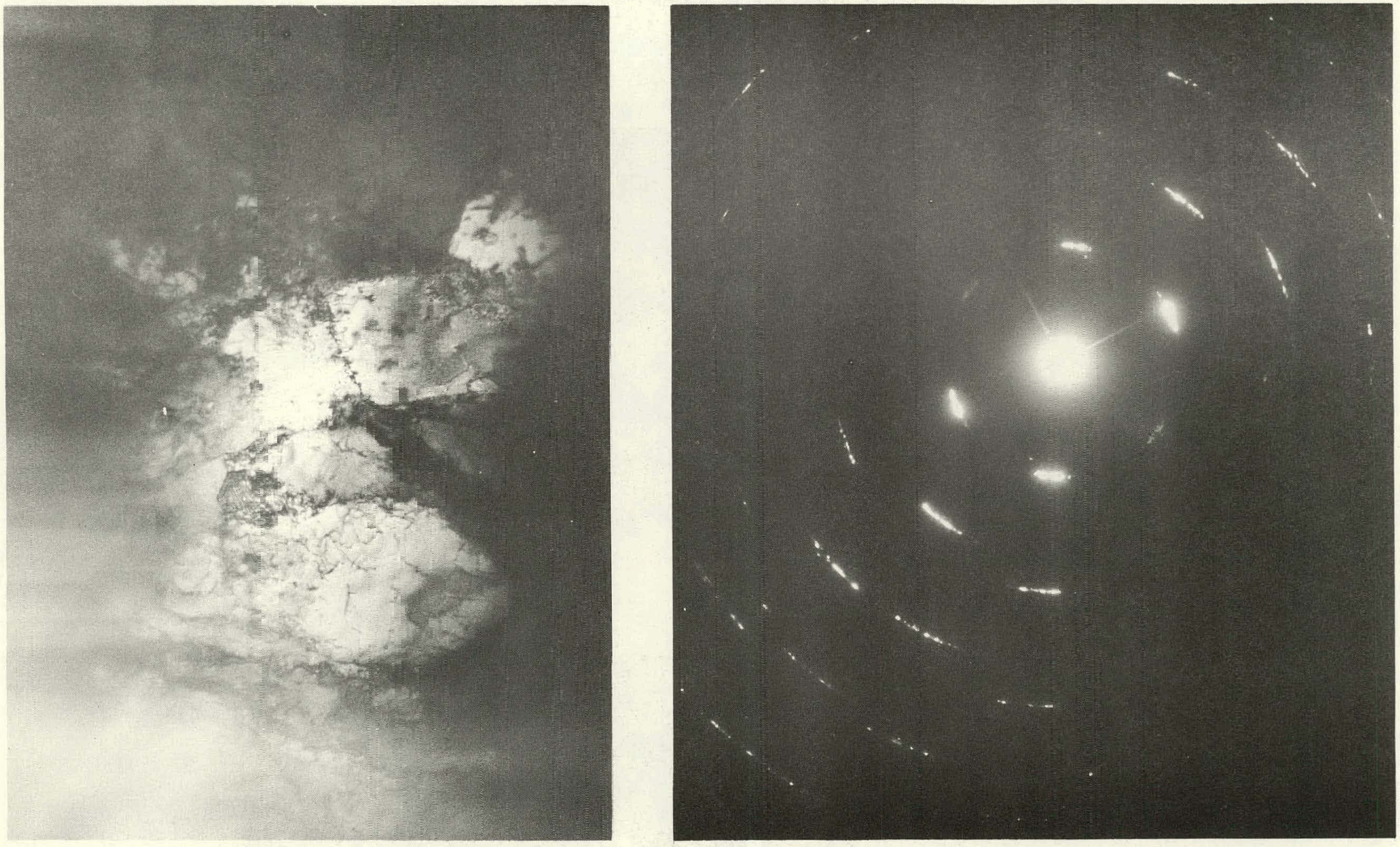

P2309 P2310

Fig. 4--Transmission micrograph of rolled tantalum single crystal after thermal treatment to pin dislocations, with selected area diffraction

P2365 (×~54,000)

Fig. 5--Transmission micrograph of rolled tantalum single crystal after thermal treatment to pin dislocations

diffraction pattern indicates that the surface of the specimen is about parallel to the (111) plane, as has also been found for cold-rolled crystals of 3% Si-Fe.(3) It was not possible to find areas in which only sharply defined spots were present--rather, a spreading out of the spots was usually present, indicating a range of orientations of the subgrains. Angular misorientations of 4° to 5° were typical and correspond with the angular misorientation of microbands seen in rolled crystals of 3% Si-Fe.(3)(4) The major difference is that no tendency toward elongation of the subgrains in the rolling direction was noted in the present work, and indeed, no evidence for subgrains was found until the thermal treatment described above. If the effect is real, it indicates a quite low temperature for rearrangement of dislocations--lower than those previously reported(3)(4) even for iron.

A possible explanation may be found in the work of J. Lothe,(5) who has postulated on theoretical grounds that impurity atoms may exert sufficient force on a dislocation line to cause it to become straight. We presently have two specimens from a rolled tantalum single crystal which will be sealed in quartz ampoules, one containing helium, the other oxygen; given identical thermal treatment; and inspected to determine whether this effect is real.

DISLOCATION DYNAMICS

In a previous report(1) it was shown that reversible plastic deformation in niobium proceeded in several stages, each stage characterized by a certain temperature for a given effective measuring strain rate. It was further shown that the temperatures of each stage closely correspond to the temperatures of the various deformation-induced internal-friction peaks described numerous times before in this study. In that report, the reversible plastic deformation was measured at a number of effective strain rates and applied stresses over a range of temperatures by simply measuring the amplitude-dependent modulus defect of the sample for various strain amplitudes and temperatures. It will be recalled that if ϵ_{dis} is the dislocation component of strain and ϵ is the elastic component of strain, then the modulus defect, $\Delta M/M$, is equivalent to the ratio ϵ_{dis}/ϵ as long as $\epsilon_{dis} << \epsilon$. Thus, the dislocation strain can be obtained as the product of the elastic strain and the modulus defect. In this manner the usual stress-strain curves of a material may be obtained for various temperatures and applied stresses by using internal-friction techniques.

The correspondence noted between the temperatures of the stages observed in the amplitude-dependent modulus defect and the deformation-peak temperatures will be more firmly established in the present report.

Figure 6 represents the internal friction versus temperature for the

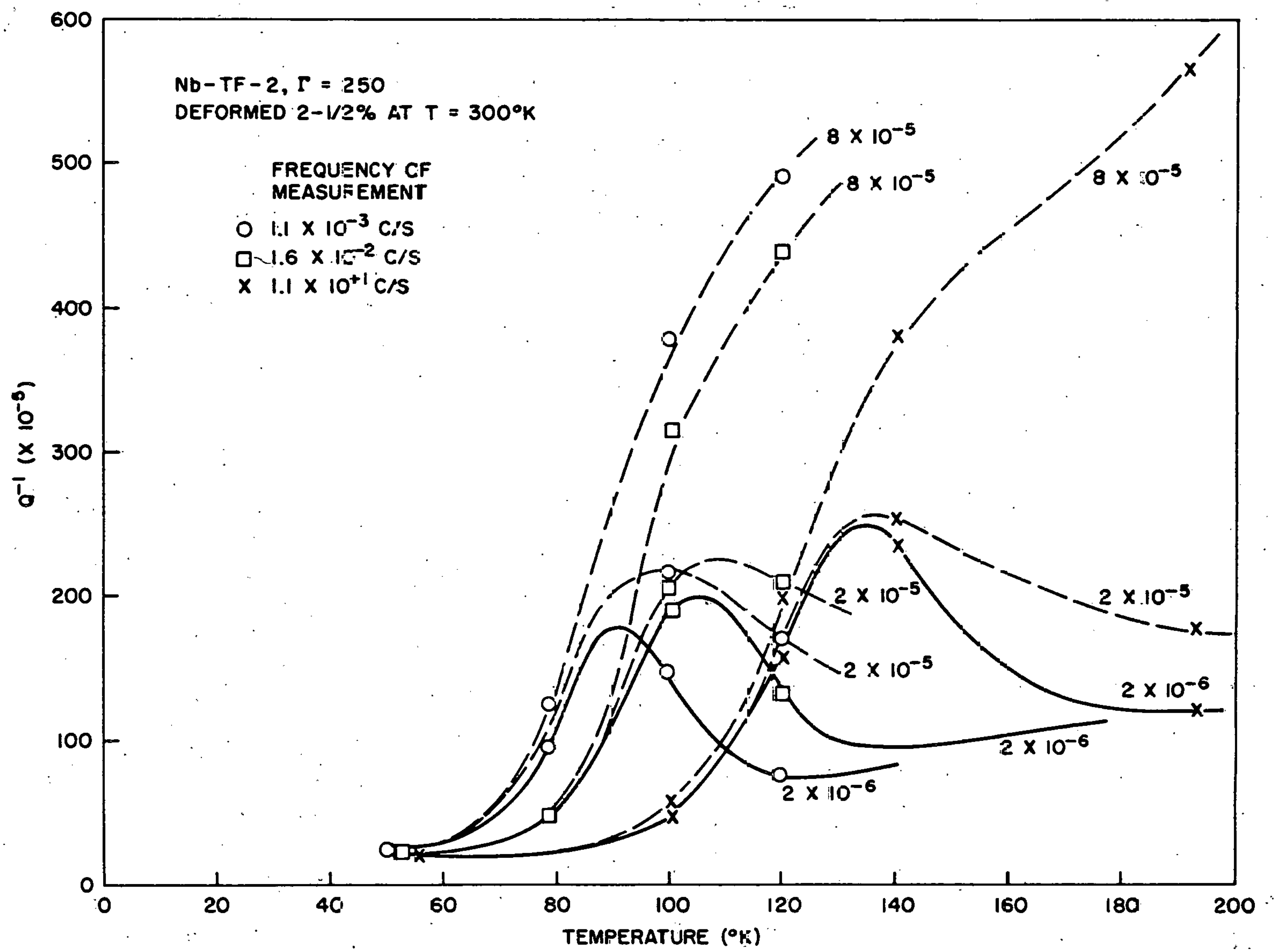

Fig. 6--Internal-friction spectrum of niobium as a function of frequency and stress amplitude

niobium specimen Nb-TF-2. This specimen was obtained from the same high-vacuum-outgassed stock of niobium wire as the previously studied Nb-TF-1; the resistance ratio, Γ, was close to 250. Nb-TF-2 was deformed in torsion 2-1/2% at room temperature, and the internal friction and modulus defect were measured from 50°K up to 193°K at three different frequencies--1.1×10^{-3}, 1.6×10^{-2}, and 11 c/s--and oscillation shear stress amplitudes of from 2×10^{-6} G up to 8×10^{-5} G, where G is the shear modulus. The various frequency and stress-amplitude measurements were made at a given fixed temperature. The two lowest frequencies were measured by the hysteresis loop method, and the 11 c/s measurement was made by the standard free decay method. Time dependence of the measurements was noted to increase strongly on passing over the α peak (135°K for 11 c/s); however, in no case was the low-amplitude measurement ever modified by the observed time effects by more than 5%. It can be seen clearly from Fig. 6 that the first stage noted earlier in the amplitude-dependent modulus defect of specimen Nb-TF-1 is also evident in the amplitude-dependent internal friction of specimen Nb-TF-2. Also, since Nb-TF-2 has been deformed several percent, the amplitude-independent α deformation peak is evident. The most important feature of these measurements is that it is clear that the temperature of the deformation peak and the temperature of the beginning of the amplitude-dependent internal friction are closely related: Thus, when the frequency of the measurement is reduced by four decades, the temperatures of both the deformation peak and the beginning amplitude-dependent stage are shifted down almost 40°K. In Fig. 7, the study of the amplitude-dependent internal friction is extended up to room temperature and to higher stress amplitudes (10×10^{-4} G) at 11 c/s. One of the most interesting points to be noted in this set of measurements is the rise in internal friction which appears in the vicinity of 50°K for stress amplitudes exceeding $\sim 2 \times 10^{-4}$ G. Also of considerable interest is the steep rise which occurs near the temperature of the amplitude-independent α peak.

The rise at 50°K appears to be associated with the increase in the relaxation strength of a group of peaks previously observed in the amplitude-independent internal-friction spectrum of moderately cold-worked niobium. This new group of peaks has been labeled the α' peaks. A similar very low-temperature peak component appears in the spectrum of molybdenum, especially in the later stages of annealing.

It is interesting to compare the difference in behavior of the amplitude-dependent internal friction on the high-temperature side of the α' peaks with that on the high-temperature side of the α peaks. In Fig. 7 it is seen that the internal friction decreases from 50°K to a minimum near 80°K for measurements exceeding 2×10^{-4} G; on the other hand, the internal friction increases monotonically for this amplitude range from 80°K upwards through the α-peak range and beyond. The monotonic rise of internal friction on the

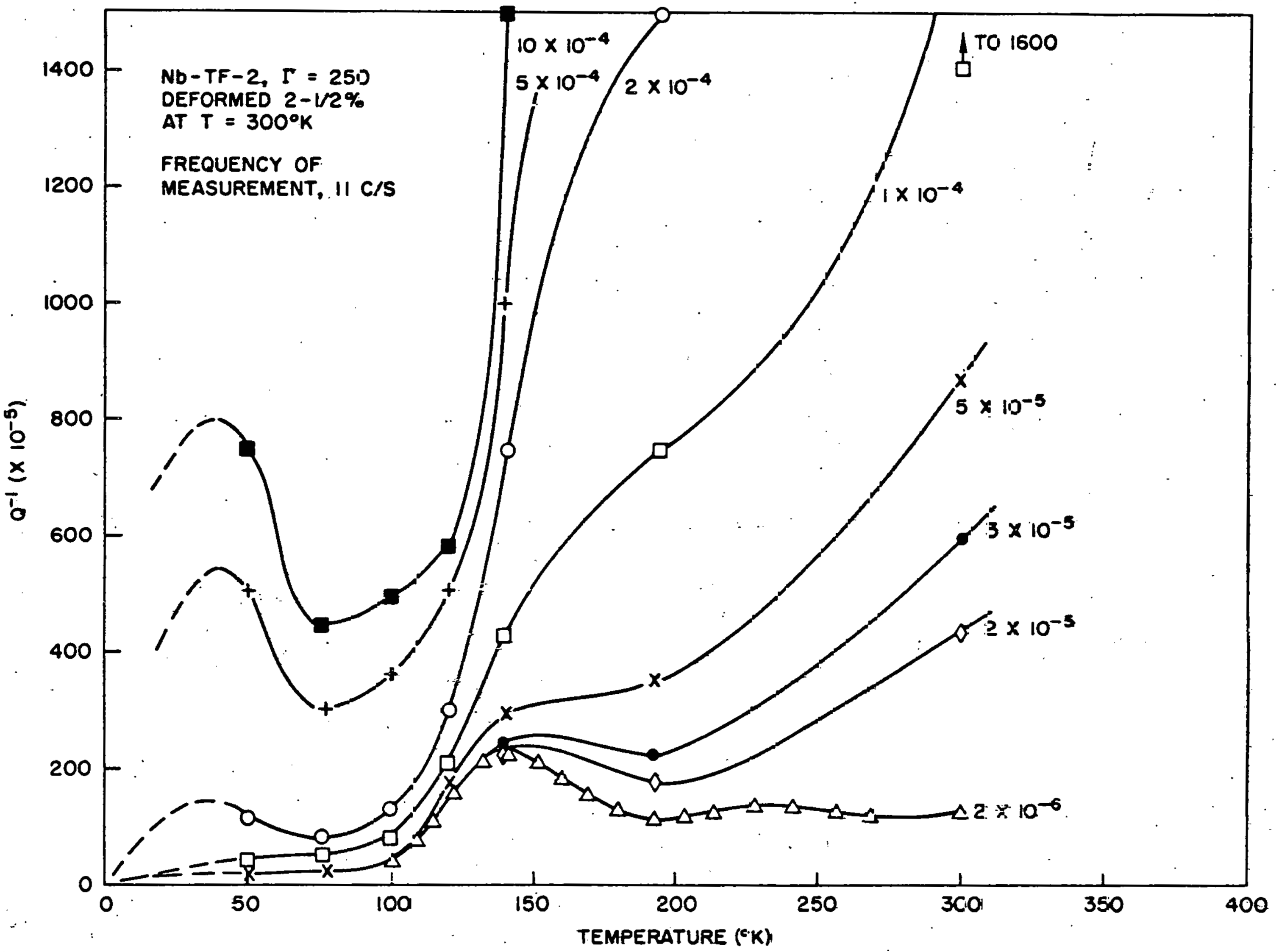

Fig. 7--Internal-friction spectrum of niobium measured at 11 c/s as a function of stress amplitude

high-temperature side of the α peak is consistent with the behavior of a hysteresis process which is coupled in series with a relaxation process, as pointed out by Chambers(6) in discussing amplitude-dependent internal friction in tantalum. The hysteresis process believed to be operating here is the breakaway of dislocations from impurity pinning points, and the series-coupled relaxation process is the thermally activated motion of the dislocation segment moving between the pinning points; thus, if, and only if, the segment is free to move can the breakaway process give rise to hysteretic internal friction. The drop in internal friction on the high-temperature side of the α' peak suggests that the increased oscillating stress acts principally to increase the relaxation strength of the α' peak.

More information can be obtained concerning the amplitude dependence of the mechanisms operating near the α' and α peaks by observing the modulus defect as a function of temperature as is shown in Fig. 8. The modulus defect was obtained by the means discussed in Ref. 1. It can be seen that the modulus defect measured at high amplitudes is less temperature dependent for temperatures near 50°K than that measured at low amplitudes, which results in the amplitude-dependent modulus defect decreasing for increasing temperatures in the temperature interval from 50° to 90°K, closely paralleling the corresponding amplitude-dependent internal-friction behavior.

Figure 8 also shows that for small oscillating stresses (2×10^{-6} G), reversible dislocation motion occurs in two stages, the first starting below 50°K and ending near 150°K ($\alpha' + \alpha$ peak) and the second starting near 200°K and ending near 300°K (β peaks). As the applied stress increases, the β process appears to increase in strength and shift toward lower temperatures. At present it seems that this apparent shift of the β-peak process can be explained by a stress-assisted increase in the hysteretic component of the β peak.

Perhaps the most important feature seen in both Fig. 7 and Fig. 8 is the role played by the α peak. At temperatures above this peak the internal friction and modulus defect increase monotonically with increasing applied stress; furthermore, the rate of increase in these quantities is seen to increase with increasing stress. On the other hand, at temperatures below the α peak the rate of increase of the amplitude-dependent internal friction and modulus defect is considerably smaller, and there is evidence of saturation near the highest stress values used in this investigation ($\sim 10 \times 10^{-4}$ G). Similar studies in tantalum show not only saturation but a definite decrease of both the internal friction and the modulus defect for stresses exceeding $\sim 3 \times 10^{-4}$ G. Since the tantalum specimens had resistance ratios of the order of ten times as great as the present niobium value, it is reasonable to conclude that the saturation stresses are related to the number of impurity pinning points, higher stresses being necessary to produce saturation in the more heavily pinned niobium.

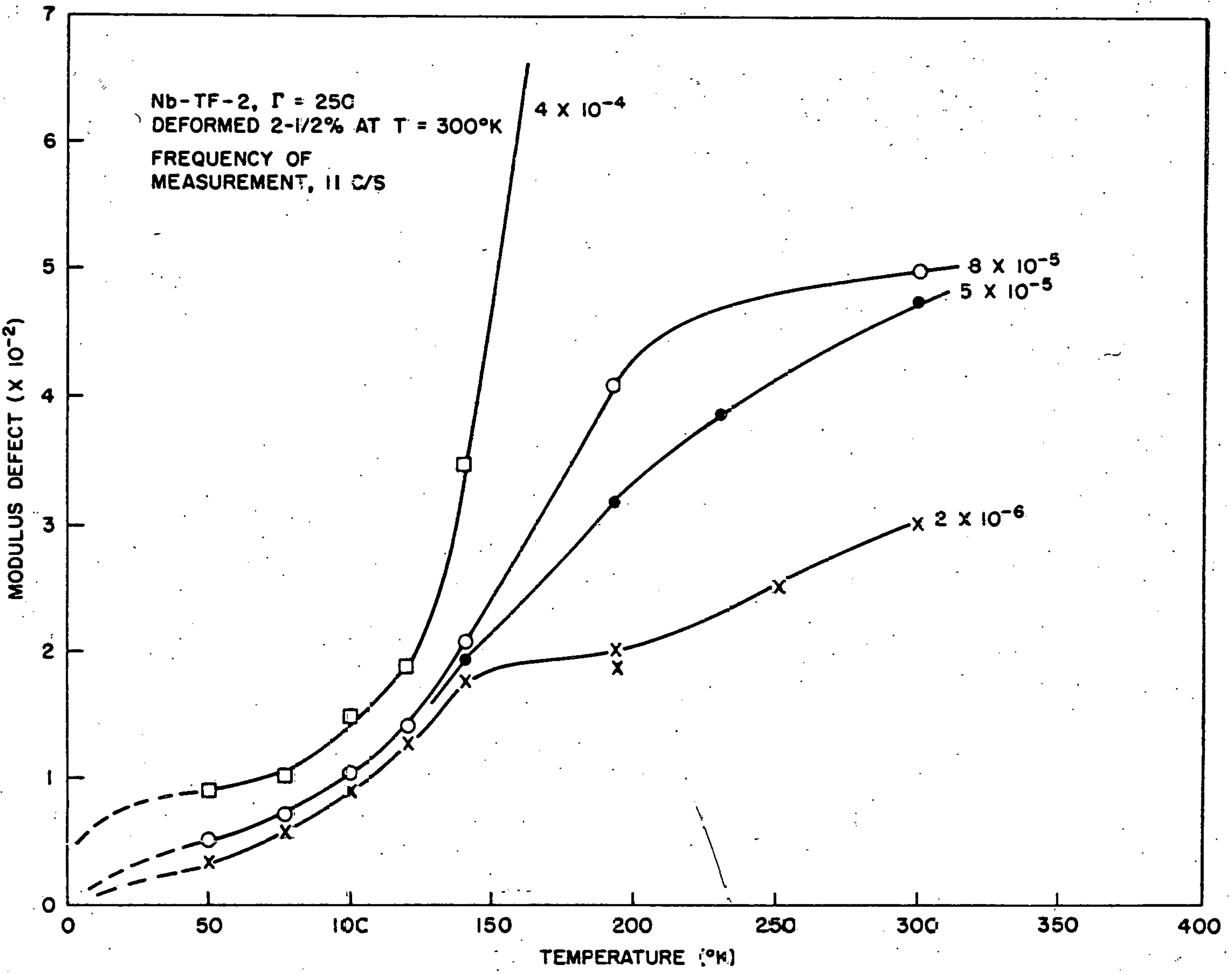

Fig. 8--Modulus-defect spectrum of niobium measured at 11 c/s as a function of stress amplitude

It can be concluded from the above experiments that much more extensive dislocation motion is possible for a given applied stress amplitude at temperatures above the α peak than at temperatures below this peak. Furthermore, limited dislocation motion is possible at temperatures far below the α peak if the applied stress is great enough. Also, at 50°K the total amount of dislocation strain possible can be estimated, from the data in Figs. 7 and 8, not to exceed about 10^{-5} at strain rates of $\sim 5 \times 10^{-4}$ sec^{-1}, whereas at temperatures just above the α peak, at least ten times as much plastic strain is observed even at higher strain rates.

From this data it is evident that the mechanism associated with the α peak plays an extremely important role in determining macroscopic plastic flow at low temperatures or high strain rates in the refractory bcc metal niobium.

II. STORED-ENERGY RELEASE IN DEFORMED METALS

The continuing aim of the present work is to investigate the effect of material and deformation variables on the stored-energy-release spectrum of deformed iron. Iron has been selected as the structural bcc metal most suitable for the calorimetric studies because recrystallization should occur within the temperature range of the differential-thermal-analysis technique, the mechanical behavior is generally characteristic of the other bcc metals, and specimens of good purity are available. Work during the past quarter included stored-energy-release measurements on Puron iron specimens of several grain sizes and at two strain levels and some preliminary measurements on another iron designated Ferrovac E.

The results provide further evidence that the stored energies, and thus the dislocation densities, in polycrystalline iron are markedly smaller than in copper and other fcc metals. There is an appreciable effect of grain size on the sharpness of the release spectrum, but calorimetric difficulties combined with the small quantities of stored energy have made it difficult as yet to obtain adequate quantitative definition of the effect of grain size on the total stored energy. The calorimetric problems have been traced to instabilities in the heaters resulting from the runs to higher temperatures, and methods for stabilizing the heating conditions are currently being tested.

CALORIMETER OPERATION

Base-line registry as satisfactory as that attained with the copper calorimeter block used in lower-temperature-range studies(7) has not yet been realized in the work with the molybdenum block. The observation of a strong dependence of the base line on temperature suggested the possibility of unsatisfactory heating conditions. An investigation of the temperature distribution by means of differential thermocouples placed at several positions on the internal walls of the calorimeter block showed that the temperature distribution was nonuniform and that the temperature sensed at the wall thermocouple (T_W) was not representative of the effective average wall temperature.

In order to establish T_W as a proper representative temperature in respect to heat flow from the block to the specimens, several taps were placed on the heater winding to enable small amounts of power to be trimmed from those sections of the block which were running hotter than the average.

The shunt was adjusted to give $T_W - T_r = 0$, where T_r is the temperature sensed at the reference specimen, when the block temperature was maintained constant at approximately 600°C.

Another difficulty encountered in extending the calorimetric measurements to higher temperature is a gradual deterioration of the alumina cement which insulates the heater winding from the molybdenum block. This deterioration has caused current leakages through the block and consequent local variations in wall temperature leading directly to base-line disregistry. Two potential solutions to this problem, the use of sheathed windings and the development of a "bird-cage" heater standing away from the block, are currently being tested to eliminate this problem of heater instability.

A preliminary calibration run using the heat of fusion of lead has been made to establish acceptable performance of the molybdenum calorimeter system. A rough value of f' = 0.06 for the thermal coupling between the specimens has been calculated from the results. This is in acceptable agreement with the value f' = 0.075 found for the copper calorimeter system employed in the previous work. (7)

STORED-ENERGY RELEASE OF DEFORMED IRON

Stored-energy-release measurements have been made on two commercial grades of pure iron: (1) Puron iron, supplied by the Westinghouse Electric Corporation, nominal analysis indicating 99.95% Fe and 30 ppm C; and (2) Ferrovac E iron, supplied by the Crucible Steel Company, nominal analysis indicating approximately 99.9% Fe and 70 ppm C. The microstructures of these materials in the annealed condition are shown in Fig. 9. The principal difference is the larger density of precipitate particles in the Puron iron.

The stored-energy release of Puron iron has been measured for three conditions of grain size and strain. A grain size of approximately 60 μ was obtained by annealing at 800°C for 30 min in helium. One of the more satisfactory measurements of the total stored energy released from a specimen of this type deformed in compression to a true strain of 41% was 2.5 (±0.7) cal/g-atom (see Fig. 10).

Fine-grained specimens of Puron iron were obtained by a process consisting of deformation by cubic compression to accumulated strains of several hundred percent followed by annealing in helium for 5 min at 550°C. The average grain size was approximately 25 μ. Calorimetric measurements on specimens deformed to true strains of 42% and 62% yielded stored-energy releases of 2.9 (±1.2) and 4.9 (±1.2) cal/g-atom, respectively.

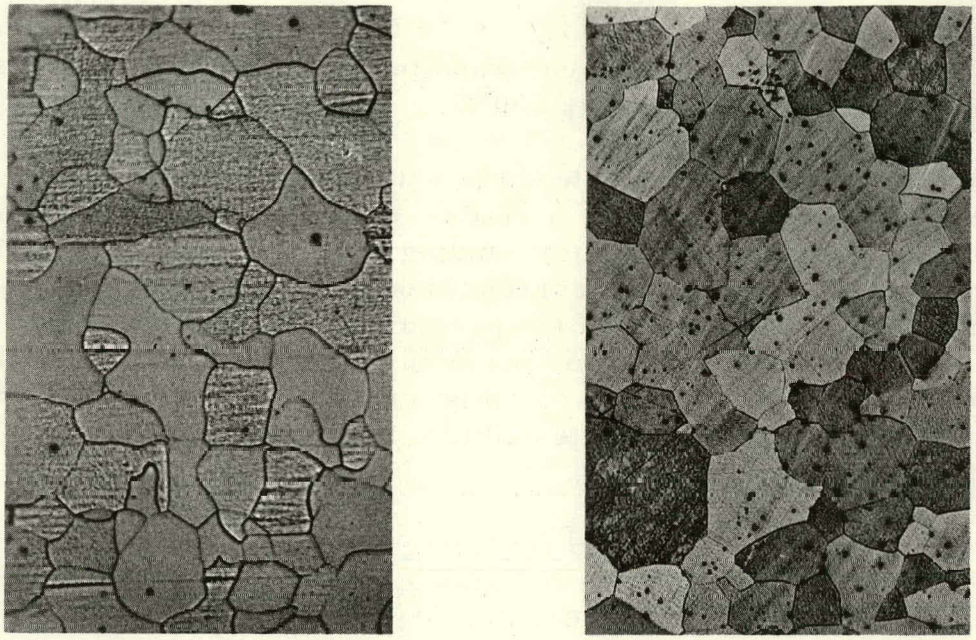

M3846-1-1 (100×)
(a)

M1822-1-1 (100×)
(b)

Fig. 9--Photomicrographs of (a) Ferrovac E iron annealed at 800°C for 12 hr and (b) Puron iron annealed at 816°C for 30 min

The stored-energy-release spectra for these experiments are given for comparison in Fig. 10. In general, the base lines were unsatisfactory and are omitted for clarity; for this reason relatively large estimates of uncertainty have been assigned to the results. However, the results indicate that the dislocation density continues to increase rapidly with strain above 40% strain and that grain boundaries cause appreciable differences in dislocation densities. Thus, the stored-energy results are in qualitative agreement with the dislocation density counts made at relatively low strains(8)(9) and provide data at higher strains where counting techniques are extremely difficult.

Several experiments have been conducted to investigate the fluctuations in the stored-energy-release curves just below 600°C. This artifact is apparently reversible, occurring in the base-line curves as well as the release curves. The initial tests with inert materials as specimens eliminated the possibility of thermal effects associated with the materials of the calorimeter system. A recent experiment in which an annealed Puron iron specimen was run as the test specimen and an annealed molybdenum specimen was run as the reference specimen showed an exothermic thermal effect of approximately 2.5 cal/g-atom occurring over the range 590° to 625°C.

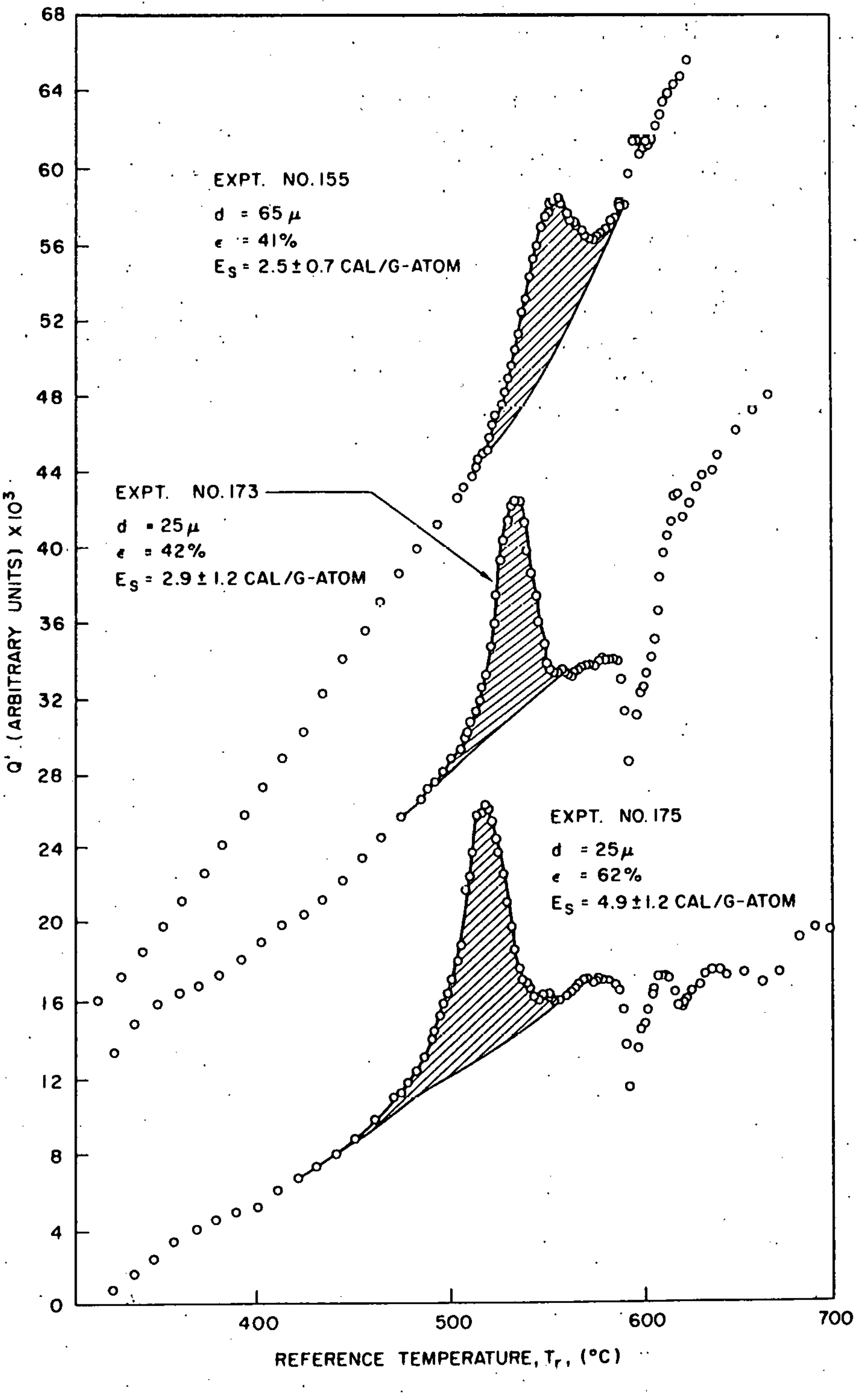

Fig. 10--Representative stored-energy-release curves for Puron iron deformed in compression: E_s = total stored energy obtained by integrating area under curve, d = average grain size, ε = true strain

Further investigations of this artifact will be made when improved heating conditions are available for the high-temperature runs desired for this work.

One measurement of stored-energy release has been made on a specimen of Ferrovac E iron. An average grain size of 55 μ was obtained by annealing at 800°C for 12 hr in helium. The specimen was deformed in compression to a true strain of 60%. The calorimeter run was made using annealed Puron as the reference, and the stored-energy-release spectrum was complicated by the fact that the recrystallization peak occurred almost simultaneously with the Puron artifact. A rough value of 2 cal/g-atom was obtained by subtracting the appropriate areas under the Ferrovac E release curve and the Puron 600°C artifact. Further measurements will be made using an inert reference material.

REFERENCES

1. T. A. Trozera, R. H. Chambers, and J. L. White, "A Program of Basic Research on Mechanical Properties of Reactor Materials," Quarterly Progress Report for the Period Ending December 31, 1962, General Atomic Report GA-3845, February 8, 1963 (22 p.).

2. I. G. Greenfield and H. G. F. Wilsdorf, "Effect of Neutron Irradiation on the Plastic Deformation of Copper Single Crystals," J. Appl. Phys. 32, 827-39 (1961).

3. Hsun Hu, "Microbands in a Rolled Si-Fe Crystal and Their Role in Recrystallization," Acta Met. 10, 1112-16 (1962).

4. J. L. Walter and E. F. Koch, "Electron Microscope Study of the Structures of Cold-rolled and Annealed (100)[001] Crystals of High-purity Silicon-Iron," Acta Met. 10, 1059-75 (1962).

5. J. Lothe, "The Effect of Temperature on Dislocations with Condensed Impurity Atmospheres. Theory of Dislocation Motion and Dislocation Break-away," Acta Met. 10, 663-70 (1962).

6. R. H. Chambers, "Thermally Activated Dislocation Motion in FCC and Refractory BCC Metals," Applied Physics Letters 2, 165 (1963).

7. J. L. White and K. Koyama, "The Application of Differential Thermal Calorimetry to Measurements of Stored-energy Release in Metals," General Atomic Report GA-2732, August 6, 1962 (32 p.) (to be published in The Review of Scientific Instruments, September, 1963).

8. A. S. Keh, "Dislocation Arrangement in α-Iron During Deformation and Recovery," in Direct Observations of Lattice Defects in Crystals, J. B. Newkirk and J. H. Wernick (eds.), Interscience, New York, 1962, p. 213.

9. A. S. Keh and S. Weissman, "Deformation Substructure in Body-Centered Cubic Metals," Chap. 5 in Electron Microscopy and Strength of Crystals, G. Thomas and J. Washburn (eds.), Interscience, New York, 1963, p. 231.